Available online at www.sciencedirect.com
SCIENCE DIRECT®
Surface Science 549 (2004) 121–133
SURFACE SCIENCE
www.elsevier.com/locate/susc

Comparative DFT study of the adsorption of 1,3-butadiene, 1-butene and 2-*cis*/*trans*-butenes on the Pt(1 1 1) and Pd(1 1 1) surfaces

Ana Valcárcel [a,b], Anna Clotet [a], Josep M. Ricart [a], Françoise Delbecq [b,*], Philippe Sautet [b]

[a] *Departament de Química Física i Inorgànica, Universitat Rovira i Virgili, Pl. Imperial Tarraco 1, E-43005 Tarragona, Spain*
[b] *Laboratoire de Chimie, UMR CNRS 5182, Ecole normale supérieure de Lyon, 46 Allée d'Italie, F-69364 Lyon Cedex 07, France*

Received 30 July 2003; accepted for publication 18 November 2003

Abstract

The interaction of 1,3-butadiene, 1-butene and 2-*cis*/*trans*-butenes on the Pt(1 1 1) and Pd(1 1 1) surfaces has been studied with density functional theory methods (DFT). The same most stable adsorption modes have been found on both metal surfaces with similar adsorption energies. For 1,3-butadiene the 1,2,3,4-tetra-σ adsorption structure is shown to be the most stable one, in competition with a 1,4-metallacycle-type mode, which is only less stable by 10–12 kJ mol^{-1}. On Pt(1 1 1) these total energy calculations were combined with simulations of the vibrational spectra. This confirms that the 1,2,3,4-tetra-σ adsorption is the most probable adsorption structure, but cannot exclude the 1,4-metallacycle as a minority species. Although similar in type and energy, the adsorption on the Pd(1 1 1) surface shows a markedly different geometry, with a smaller molecular distortion upon adsorption. The most stable adsorption structure for the butene isomers is the di-σ-mode. Similarly to the case of the 1,3-butadiene, the adsorption geometry is closer to the gas phase one on Pd than on Pt, hence explaining the different spectroscopic results, without the previously assumed requirement of a different binding mode. Moreover the present study has shown that the different selectivity observed on Pt(1 1 1) and Pd(1 1 1) for the hydrogenation reaction of butadiene cannot be satisfactory explained by the single comparison of the relative stabilities of 1,3-butadiene and 1-butene on these metals.
© 2003 Elsevier B.V. All rights reserved.

Keywords: Density functional calculations; Chemisorption; Alkenes; Metallic surfaces; Platinum; Palladium

1. Introduction

The chemical industry needs unsaturated hydrocarbons in order to obtain finished products as polymers or artificial textiles. The selective hydrogenation of dienes in monoolefines has received considerable attention since this process plays a key role in manufacturing high-purity alkene streams [1]. The main example of this reaction is the 1,3-butadiene hydrogenation. The active components of the catalyst are usually noble metals, such as palladium or platinum. High selectivity for the partially hydrogenated product (mainly 1-butene)

* Corresponding author. Tel.: +33-47-244-5352; fax: +33-47-244-5399.
E-mail address: delbecq@catalyse.cnrs.fr (F. Delbecq).

0039-6028/$ - see front matter © 2003 Elsevier B.V. All rights reserved.
doi:10.1016/j.susc.2003.11.036

is obtained in the case of a palladium catalyst while platinum is less active and moreover less selective [2–6]. The lower activity and the poorer selectivity of the Pt surface in relation to the Pd one where ascribed to both the different adsorption strength and adsorption mode of 1,3-butadiene and butenes. Consequently, an accurate characterisation of the surface species seems to be a necessary step towards understanding subsequent surface processes.

A rather detailed knowledge of the surface chemistry of C_2 [7–16] and C_3 [17–20] hydrocarbons has been achieved. Nevertheless, for larger molecules, such as 1,3-butadiene and butenes, an accurate description of the adsorption remains still challenging although some experimental [6,21–28] and theoretical [29–32] studies have been focused on this problem.

At low temperatures (<95 K), 1,3-butadiene was found to be loosely bonded to both Pt and Pd surfaces [6,27]. At higher temperatures, Avery and Sheppard [24] by means of electron energy loss spectroscopy (EELS) suggested the presence of two different adsorption modes (1,2-di-σ-adsorption and 1,2,3,4-tetra-σ-adsorption) for this molecule on Pt(1 1 1). The di-σ picture of the interaction was supported by some experimental [6,25] and theoretical [30,31] works. More recent studies [27] pointed out a 1,4-di-σ-adsorbed molecule (metallacycle). Such a structure was in agreement with theoretical considerations issued from qualitative molecular orbital calculations [29]. On the Pd(1 1 1) surface, UPS and NEXAFS experiments [6,27] proposed a di-π-adsorption mode near room temperature.

The picture for the various butene isomers is less ambiguous. At low temperatures, 1-butene and 2-*cis*/*trans*-butenes are di-σ-bonded to the clean Pt(1 1 1) surface, as suggested by EELS, TDS, UPS and NEXAFS experiments [6,23–28]. Around room temperature, all these species desorb or transform into a more dehydrogenated molecule. On palladium, 1-butene is proposed to be π-bonded at temperatures under 200 K. Like on Pt(1 1 1), at higher temperatures, this molecule desorbs [6,27]. Unfortunately, to our knowledge no data is available for the 2-butene isomers adsorbed on the Pd(1 1 1) surface.

Some of us had already carried out Extended-Hückel calculations for 1,3-butadiene on Pt(1 1 1), Pd(1 1 1) [31] and Pd–Ni bimetallic systems [32]. In order to give a more quantitative approach, we have undertaken this work with first-principle calculations. The main purpose of the present study is to determine and compare the geometry, binding site preference and adsorption energies of 1,3-butadiene (C_4H_6), 1-butene and 2-*cis*/*trans*-butenes (C_4H_8) on the Pt(1 1 1) and Pd(1 1 1) surfaces by means of periodic density functional theory (DFT) calculations. Additionally, we have calculated the vibrational spectra of adsorbed species to correlate with the experimental data and help to discriminate between the possible adsorption modes. Just before submitting this article, a similar study on adsorption of unsaturated molecules on Pt and Pd surfaces was brought to our attention [33].

2. Computational method

The calculations have been performed in the framework of DFT using the Vienna Ab Initio Simulation Program (VASP) [34–36]. This program solves the Kohn–Sham equations of the DFT with the development of the one-electron wave function in a basis of plane waves. The electron–ion interactions are described by the projector augmented wave method (PAW). The PAW method is a frozen core approach, which uses the exact valence-wave functions instead of pseudo-wave functions [37]. The tight convergence of the plane-wave expansion was obtained with a cut-off of 400 eV. The generalised gradient approximation (GGA) has been used with the functional of Perdew and Wang [38]. For our purposes, four different unit cells have been considered: $\sqrt{3}\times\sqrt{3}$, 2×2, 3×2 and 3×3 respectively associated with molecular coverages of 1/3, 1/4, 1/6, 1/9 ML. The 2D Brillouin integrations have been performed on a $5\times5\times1$ grid for the $\sqrt{3}\times\sqrt{3}$ and 2×2 structures, on a $3\times5\times1$ grid for the 3×2 and on a $3\times3\times1$ grid for the 3×3 unit cells. We tested that this density of k-points gives a correct convergence of the adsorption energy in the case of the 3×3 unit cell with a difference of 0.05 eV between the

$3\times3\times1$ and $5\times5\times1$ grids. The energy differences among various adsorption modes are not modified at all when the grid is changed. The Pt(1 1 1) and the Pd(1 1 1) surfaces have been modelled by a two-dimensional slab in a three dimensional periodic cell generated by introducing a vacuum width in the direction perpendicular to the surface ($\sim$11 Å). Some tests have been performed to investigate the effect of the slab thickness on the calculated energies. In agreement with a previous study [39], the comparison between four-layer and six-layer slabs showed us that the results are consistent only when the k-point convergence is reached, the six-layer model needing a larger grid. In the present work the surfaces have been modelled by slabs containing four atomic metal layers with the hydrocarbon molecules adsorbed on one side of the slab. The Pt–Pt and Pd–Pd interatomic distances have been optimised to 2.82 and 2.80 Å for the bulk.

The geometry optimisation includes all degrees of freedom of the adsorbates and the two uppermost metal layers, while the two lowest metal planes are kept fixed at the bulk geometry. The adsorption energy (E_{ads}) is calculated as the difference between the energy of the adsorbed molecule ($E_{adsorbate\text{-}surface}$) and the sum of the free surface ($E_{surface}$) and the gas-phase molecule ($E_{gas\text{-}phasemolecule}$) energies using

$$E_{ads} = E_{adsorbate\text{-}surface} - E_{surface} - E_{gas\text{-}phase\ molecule}$$

A negative value indicates an exothermic chemisorption process. In order to compare the adsorption energies at different coverages, the energy per surface atom has to be taken into account. This is a standard procedure to normalise the energy to a given surface area. The energy per surface atom was obtained by multiplying E_{ads} by the surface coverage θ.

The frequencies and the corresponding modes have been calculated within the harmonic approach. The Hessian dynamical matrix has been obtained by numerical differentiation of the forces and diagonalized, providing the harmonic molecular frequencies and the associated normal modes. The coupling of the molecular vibrations and the surface phonons has been neglected in order to simplify the treatment. The dynamic dipole moments of the vibrational modes $d\mu/dQ_k$ have been calculated to estimate the intensities of the EELS spectra. In the specular mode, only those vibrational modes that give rise to an oscillating dipole perpendicular to the surface are active. The calculation of the derivatives of the dipole moment has been performed by finite differences from the same structures used in the frequency calculations [40]. Then the absolute intensities I_{loss} of the energy losses normalised to the elastic peak intensity $I_{elastic}$ have been evaluated following the formula in [41]

$$\frac{I^k_{loss}}{I_{elastic}} = \left(\sum_{i=1}^{3N} \frac{P_{ki}}{\sqrt{m_i}} \frac{d\mu_z}{d\Delta r_i}\right)^2 \frac{F(v_k)}{v_k}$$

where μ_z is the z-component of the dipole moment, v_k is the frequency associated to a given normal mode Q_k, $P_{ki}/\sqrt{m_i}$ is the mass weighted coordinate matrix of the normal mode and $F(v_k)$ is a function of the frequency and some fixed experimental parameters [23]. The numerical calculation of the first derivative of the dipole moment has been performed in the cartesian coordinate system (Δr_i).

The temperature and pressure diagrams have been calculated by a simple thermodynamical model [42] where the gas phase plays the role of a reservoir in equilibrium with the substrate and the adsorbed phase. Then the gas phase imposes its pressure and temperature to the adsorbed one. Only the chemical potential of the gas phase reference is explicitly considered. The effects of the pressure and temperature of the metallic substrate have been neglected.

3. Results

3.1. Adsorption on Pt(1 1 1)

First, for sake of comparison, the geometry of the gas phase molecules has been optimised. In order to avoid lateral interactions between periodic images a large box ($15\times15\times20$ Å^3) has been taken as unit cell. The results for the 1,3-butadiene molecule are close to the ones in previous experimental [43] and theoretical [44] studies. Our calculations predict a C–C distance of 1.45 Å, a C=C of 1.34 Å and a CCC angle of $\sim$124° for the *trans*-1,3-butadiene molecule. The values for the *cis*

isomer are 1.46, 1.34 Å and ~125°, respectively. For the 1-butene and 2-*cis*/*trans*-butenes the C–C distances are within 1.50–1.52 Å and the double bonds are in the interval 1.33–1.34 Å.

The adsorption energies at four different coverages are given in Table 1 for the species studied. Only the 3×3 unit cell ($\theta = 1/9$) has been used for all the molecules and structures. The influence of the adsorbate coverage has been studied for the most stable structures and for the adsorption modes proposed in previous works. Various adsorption structures were considered and optimised. We use the standard notation (π, di-σ...) and straightforward extensions. This notation is not directly linked to the hybridisation state of the carbon atoms but indicates how the double bonds of the molecule are bound to the surface, i.e. Pt–C bonds with the same metal atom for π and with neighbouring ones for di-σ. The minima obtained for the 1,3-butadiene molecule are shown in Fig. 1. The different adsorption structures are named as di-σ (Fig. 1(a)), di-π-*cis* (Fig. 1(b)), di-π-*trans* (Fig. 1(c)), 1,2-di-σ-3,4-π (Fig. 1(d)), 1,4-di-σ-2,3-π (Fig. 1(e)) and 1,2,3,4-tetra-σ (Fig. 1(f)). Only in the di-σ adsorption mode the carbon chain is not parallel to the metal surface. In this mode the molecule interacts with two surface metal atoms through one of its double bonds while the rest of the hydrocarbon points upward the metal surface. The two di-π adsorption configurations are characterised as bound to the metal surface via their two C=C bonds. The nature of the molecule–surface interaction is the same in both di-π adsorption structures. The difference resides in the conformation of the adsorbed molecule (*cis* vs. *trans*). In the 1,2-di-σ-3,4-π, again the two C=C bonds are involved in the interaction with the metal surface but not in the same way. One of the double bonds interacts with two neighbouring metal atoms while the other is bound to a single surface atom. The nature of the carbon–metal interactions in the 1,4-di-σ-2,3-π is similar to the one described for the 1,2-di-σ-3,4-π adsorption mode but a redistribution of π electron system takes place during the adsorption process. The middle C–C bond gains double bond character at expenses of the terminal ones. The molecule forms two bonds through the terminal C atoms and a π-interaction via its central C–C bond. Finally, in the 1,2,3,4-tetra-σ-adsorption mode, the molecule has a *trans* conformation and interacts with the metal surface via all its C atoms.

Table 1
Adsorption energies (kJ mol^{-1}) for the various chemisorption structures of 1,3-butadiene, 1-butene and 2-*cis*/*trans*-butene on Pt(1 1 1), as a function of the coverage

θ	1/3	1/4	1/6	1/9
1,3-butadiene				
di-π-*cis*				−114(−13)
di-π-*trans*			−110(−18)	−122(−14)
di-σ	−45(−15)	−78(−20)	−85(−14)	−89(−10)
1,2-di-σ-3,4-π		−75(−19)	−122(−20)	−140(−16)
1,4-di-σ-2,3-π			−137(−23)	−150(−17)
1,2,3,4-tetra-σ			−156(−26)	−160(−18)
1-butene				
π				−66(−7)
di-σ	−45(−15)	−83(−21)	−91(−15)	−93(−10)
2-cis-butene				
π				−58(−6)
di-σ				−80(−9)
2-trans-butene				
π				−48(−5)
di-σ				−79(−10)

The adsorption modes are those shown in Figs. 1 and 3. The values in parenthesis are the adsorption energies per surface metal atom.

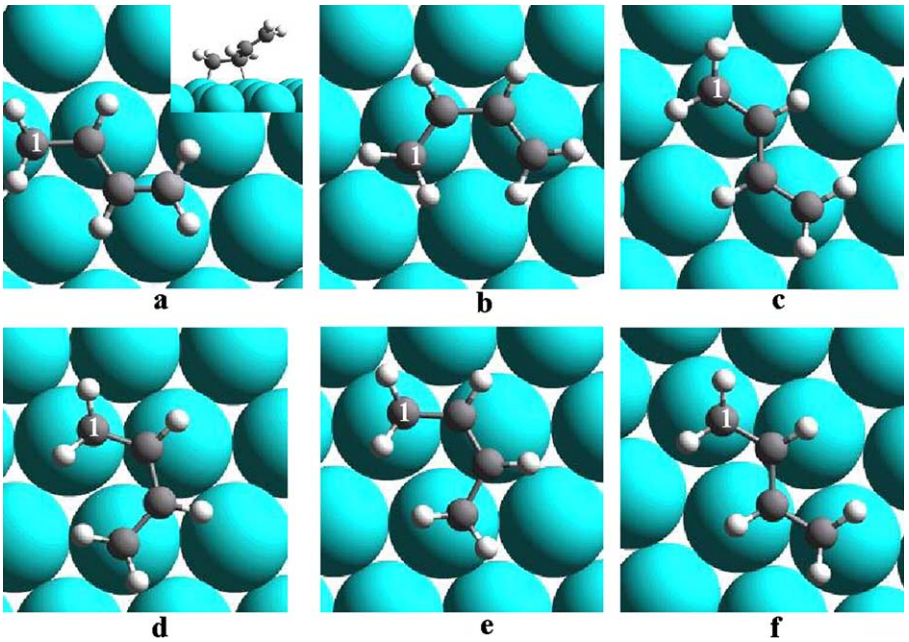

Fig. 1. Adsorption modes for 1,3-butadiene on Pd and Pt(1 1 1) metal surfaces. di-σ (a), di-π-*cis* (b), di-π-*trans* (c), 1,2-di-σ-3,4-π (d), 1,4-di-σ-2,3-π (e) and 1,2,3,4-tetra-σ (f). Carbon atom number 1 is displayed for clarity.

Among all the structures tested, the most stable adsorption mode is the 1,2,3,4-tetra-σ one (Fig. 1(f)). The 1,4-di-σ-2,3-π (Fig. 1(e)), also called metallacycle [27,29], is however only 10 kJ mol^{-1} less stable. Hence, considering the approximations for the evaluation of exchange-correlation terms in GGA-DFT, the presence of a metallacycle adsorption mode on the surface cannot be excluded on the basis of total energy. The di-σ-adsorption mode is farther apart (71 kJ mol^{-1}) from the most stable structure and hence can be clearly rejected. These results contradict previous EHT calculations [31] that pointed to the di-σ adsorption mode as the most stable one on the Pt surface. Three more minima have been found for the 1,3-butadiene molecule on the Pt(1 1 1) surface: the di-π, *cis* and *trans*, and the 1,2-di-σ-3,4-π adsorption modes (Fig. 1(b)–(d)). The two π adsorbed modes (di-π-*cis* and di-π-*trans*) have similar adsorption energies and geometries (see Tables 1 and 2). These surface structures are less stable than the tetra-σ adsorption mode by 46 and 38 kJ mol^{-1} respectively. The 1,2-di-σ-3,4-π adsorption mode is only 20 kJ mol^{-1} less stable than the 1,2,3,4-tetra-σ one.

The computed adsorption energies, using the same methodology, for ethylene and propylene are ∼−104 and ∼−91 kJ mol^{-1} [45] respectively, that can be compared with the present results of −93 kJ mol^{-1} for 1-butene and −80 kJ mol^{-1} for 2-butene. Note that the adsorption energy decreases with the number of substituents on the double bond, propene and 1-butene having a similar value. The methyl substituents have two effects on the molecular adsorption. From their electron donating character, they shift up in energy the π molecular orbitals of ethylene. The π* orbital is hence moved further away from the top of the d band, decreasing the back-bonding interaction and the adsorption strength. The second effect is an increased Pauli repulsion between occupied orbitals of the molecules and the surface, resulting in a larger steric effect [46]. For 1,3-butadiene, the interaction energy is −160 kJ/mol. This is less than twice the adsorption energy of 1-butene or ethylene. In this case, in addition to steric effects, the resonance stabilizing the gas phase butadiene lowers the binding energy. This effect has also been reported for the interaction energy of benzene on

Table 2
Geometrical parameters for the adsorption structures of 1,3-butadiene, 1-butene and 1-*cis*/*trans*-butene on Pt(1 1 1) for a coverage of $\theta = 1/9$-ML

	PtC_1	PtC_2	PtC_3	PtC_4	C_1C_2	C_2C_3	C_3C_4
1,3-butadiene							
di-π-*cis*	2.17	2.25	2.23	2.17	1.42	1.47	1.42
di-π-*trans*	2.18	2.22	2.23	2.17	1.42	1.46	1.42
di-σ	2.11	2.17	[2.90]	[3.81]	1.49	1.47	1.35
1,2-di-σ-3,4-π	2.11	2.17	2.33	2.16	1.49	1.46	1.42
1,4-di-σ-2,3-π	2.10	2.26	2.26	2.10	1.48	1.43	1.48
1,2,3,4-tetra-σ	2.10	2.18	2.18	2.11	1.48	1.48	1.48
1-butene							
π	2.19	2.23	[2.61]	[4.01]	1.41	1.51	1.54
di-σ	2.12	2.14	[3.05]	[4.45]	1.49	1.52	1.54
2-cis-butene							
π	[3.48]	2.24	2.24	[3.44]	1.50	1.42	1.50
di-σ	[3.02]	2.15	2.15	[3.02]	1.52	1.50	1.52
2-trans-butene							
π	[3.21]	2.23	2.23	[3.24]	1.50	1.42	1.50
di-σ	[3.03]	2.13	2.13	[3.03]	1.52	1.50	1.52

Distances are in Å. The numbers in brackets account for the longer distance between two atoms not directly bound.

Pt(1 1 1) [39]. The computed binding energy was around −88 kJ/mol, much lower than three times the adsorption energy of ethylene.

The calculation of the adsorption energies per surface atom (Table 1, numbers in brackets) concludes that the most stable adsorbed phase for the 1,3-butadiene at 0 K is the 1,2,3,4-tetra-σ adsorption mode in a 1/6 ML coverage. One has to take into account that flat structures, like 1,2,3,4-tetra-σ or 1,4-di-σ-2,3-π modes, cannot exist at high coverages due to steric effects. In order to complete our results, the temperature and pressure phase diagrams have been calculated. At a given pressure (UHV) the most stable phase around 150 K is the 1,2,3,4-tetra-σ adsorption mode in a 1/6-ML coverage. As the temperature increases (220 K) the 1/9-ML layer becomes the most favoured adsorbed phase. No crossing between two different adsorption modes is observed. At higher pressures (reaction conditions), the same behaviour is found but the transition temperature between 1/6 and 1/9-ML is shifted to a higher value.

The characteristic bond lengths for the adsorbed structures are given in Table 2. For all the species studied the Pt–C bonds are in the range 2.10–2.33 Å, which corresponds to the usual values obtained in organometallic complexes [47]. The C–C bonds involved in the adsorption are elongated with respect to the gas phase except for the C–C central bond of the 1,4-di-σ-2,3-π structure that gains double bond character and is shortened during the adsorption processes. The C–C bond length has been used as a measure of the activation of the adsorbed molecule. One observes that the C–C bond is more elongated for the di-σ geometries than for the π ones, in relation to the stronger adsorption. The most stable structure for the 1,3-butadiene on the Pt surface presents a large expansion of its C–C bonds (1.48 Å). This value is not far from the usual distance for a C–C single bond (1.54 Å) and is in good agreement with the C–C distance found for the ethene molecule on Pt in previous experimental [48] and theoretical [11,45] studies. This indicates the σ nature of the bonding and an important reduction in the double bond character. The fact that the three C–C bonds are equal indicates that they acquire the same character upon adsorption. The σ interaction is accompanied by a rehybridisation towards sp^3 with a C–CH_2 angle reduced to ∼132° compared to the value of 180° for an alkene and it is close to the characteristic value in alkanes (125°). On the

adsorption modes named as di-π the values of the C–CH_2 angles are only slightly apart from the sp^2 hybridisation ones (∼157°).

Since the total energy calculations do not allow a clear cut discrimination between the two most stable structures (1,2,3,4-tetra-σ and the metallacycle), the simulation of vibrational spectra from first principles is a key tool to obtain additional information and a direct comparison between calculated and measured data. No information about the coverage is available in the experimental sources [23,24]. The calculation of the simulated spectra has been performed for the most stable system obtained in our calculations (1/6-ML). As a reference, the frequencies of the gas phase 1,3-butadiene have been also calculated. Table 3 shows the obtained values and the experimental ones [44,49]. The good agreement between the computed and the experimental values validates the theoretical approach used to calculate the vibrational frequencies. However we remark that frequencies are calculated in the harmonic approximation and they are not scaled. Usually pure DFT frequencies agree very well with experimental frequencies [50] although C–H stretching frequencies are slightly overestimated due to anharmonic effects [51,52]. The approximate description of the C–H stretching region is not a hindrance because this part of the spectrum does not hold the subsequent analysis. Regarding our results for free 1,3-butadiene, the errors are below 2% except for the highest $\nu(CH_2)$ asym. and the lowest δ(C=C–C) and τ(C–C) frequencies.

Table 3
Vibrational frequencies of the gas phase 1,3-butadiene molecule

Experimental	Computed	Assignment
3100	3217	$\nu(CH_2)$ asym.
3100	3179	$\nu(CH_2)$ asym.
3055	3122	ν(CH)
3013	3049	$\nu(CH_2)$ sym.
3010	3035	$\nu(CH_2)$ sym.
3013	3007	ν(CH)
1644	1647	ν(C=C) sym.
1597	1600	ν(C=C) asym.
1441	1428	$\delta(CH_2)$ sym. sci.
1381	1372	$\delta(CH_2)$ asym. sci.
1291	1286	δ(CH)
1295	1272	δ(CH)
1203	1196	ν(C–C)
1014	1029	γ(CH)
965	970	γ(CH)
990	968	$\rho(CH_2)$ asym.
908	905	$\omega(CH_2)$ asym.
908	901	$\omega(CH_2)$ sym.
888	877	$\rho(CH_2)$ sym.
752	762	$\tau(CH_2)$ asym.
525	535	$\tau(CH_2)$ sym.
512	502	δ(C=C–C) sym.
291	270	δ(C=C–C) asym.
163	184	τ(C–C)

Values in cm^{-1}. Experimental values from Ref. [44].

Fig. 2 shows the experimental [24], and calculated vibrational spectra for the adsorbed 1,3-butadiene molecule. Fig. 2(b)–(d) correspond to 1,2,3,4-tetra-σ, metallacycle and di-σ structures respectively. The experimental EELS spectrum shows a large number of bands with an intensity larger than ∼1/3 of the most intense one at 780 cm^{-1}: the CH stretching bands around 2900–3000 cm^{-1} and several peaks at 1430, 1360, 1180, 1055, 900 and 430 cm^{-1} [53]. Later HREELS works on the same system [6,27] are quite comparable to this spectrum obtained by Avery and Sheppard [24].

The spectrum for the tetra-σ mode (Fig. 2(b)) matches very well with the experimental data, with shifts in the calculated frequencies of 5–30 cm^{-1} and a fair agreement in the intensities. The main peaks present in the experimental spectrum appear also in the theoretical one: 1418, 1403, 1148, 1058, 900, 788 and 370 assigned to the δ sci CH_2 (scissoring) of C1, δ sci CH_2 (scissoring) of C4, ρ CH_2 (rocking), ν C–C (stretching), χ CH symmetric (deformation out of plane), τ CH_2 asymmetric and ν Pt–C totally symmetric modes. Only the peak at 370 cm^{-1} is slightly far away from the experimental one, but this can be the result of computational limitations for low frequency modes. Considering the intensities, the peak at 1055 cm^{-1} (exp) is formed by the superposition of several calculated bands and the relative calculated intensity for the main peak at 780 cm^{-1} (exp) appears somewhat underestimated.

The spectrum for the metallacycle adsorption mode is much less balanced and shows a dominant peak at 834 cm^{-1} assigned to the χ CH symmetric mode (out of plane deformation). Taking into account the finite experimental resolution, this peak could overlap with the band at 780 cm^{-1} and

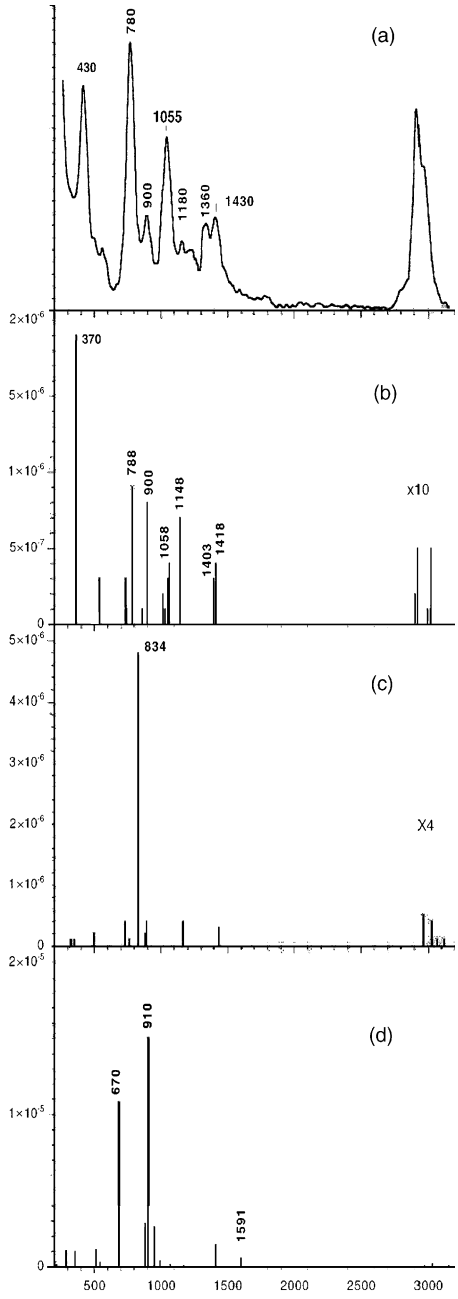

Fig. 2. Vibrational spectra of 1,3-butadiene chemisorbed on Pt(1 1 1). Experimental EELS spectrum reproduced from 24 (a), 1,2,3,4-tetra-σ (b), 1,4-di-σ-2,3-π (metallacycle) (c) and di-σ (d) adsorption modes. Simulated spectra have been calculated for a coverage of 1/6-ML. Frequencies in cm^{-1}. Intensities of the calculated spectra in arbitrary units. Notation ×10 and ×4 on figures (b) and (c) account for relative scales. Values with respect to the di-σ spectrum (d).

increase its intensity. However the total absence of intense modes for this metallacycle structure around 1000 cm^{-1}, and more generally the small relative intensity of all other peaks of the spectrum compared to the dominant one at 834 cm^{-1}, indicates that this structure cannot be the majority species on the surface.

The spectrum of the di-σ adsorption mode (Fig. 2(d)) is clearly dominated by the features at 670 and 910 cm^{-1}. Compared to these intense peaks, bands in the regions of 300, 1000 and 3000 cm^{-1} are *quasi*-negligible. For all these reasons and the presence of a peak at 1591 cm^{-1} assigned to the ν C=C, the agreement with the experimental spectrum is very poor. Therefore, considering both the relative stabilities in the total energy calculations and the comparison between simulated spectra and the experimental ones [6,24,27], we propose that the 1,2,3,4-tetra-σ mode is the most probable adsorption structure. The metallacycle structure could however be present on the surface as a minority species. This would explain the enhance intensity for the peak at 780 cm^{-1} compared to that simulated for the 1,2,3,4-tetra-σ structure alone.

In order to get a first insight into the surface processes, the adsorption of 1-butene and 2-*cis*/*trans*-butenes on the Pt(1 1 1) surface has been tackled. Various conformations of the ethyl group have been considered in the case of the 1-butene. Table 1 also shows the adsorption energies for the three isomers. The picture is obviously simpler for butenes than for the butadiene molecule. Only a π or a di-σ interaction is possible for these molecules (see Fig. 3). For all the isomers the di-σ adsorption mode is unambiguously the preferred one on the Pt(1 1 1) surface. In contradiction with previous studies [2,3,6,25,27,31] that pointed to a similar stability for both 1,3-butadiene and 1-butene, our calculations predict an adsorption energy smaller for the monoalkene than for the diene molecule (−93 vs. −160 kJ mol^{-1}). The study of the relative stability of the surface species as a function of the temperature confirms that at a given pressure the 1,3-butadiene is always more strongly adsorbed than the monoalkene. If the energy per surface unit is considered, the 1/4-ML turns out to be the best-adsorbed phase for the 1-butene molecule on the Pt surface.

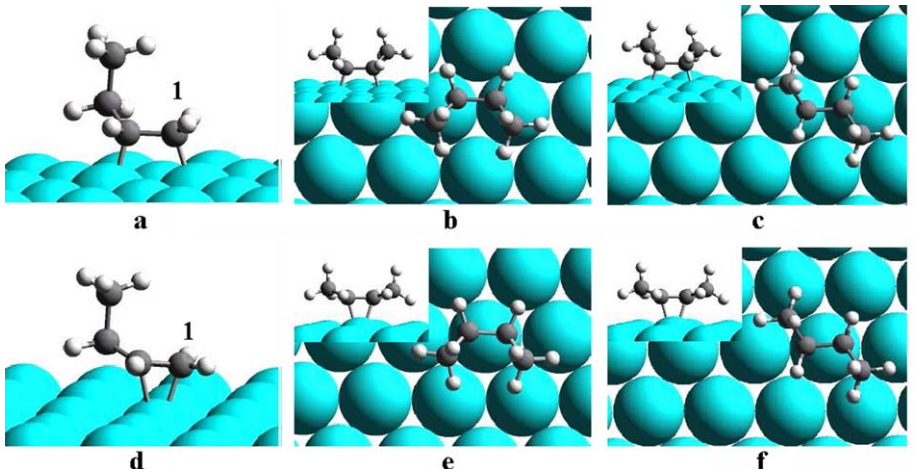

Fig. 3. Adsorption modes for 1-butene and 2-*cis*/*trans*-butenes on Pd and Pt(1 1 1) metal surfaces. (a)–(c) correspond to the di-σ-adsorption mode for 1-butene, 2-*cis*-butene and 2-*trans*-butene, respectively. The π-adsorption mode for the three isomers is depicted in (d)–(f).

The analysis of the geometrical parameters presented in Table 2 shows the same trend as observed for the 1,3-butadiene molecule. The molecules interact with the metal surface through their C=C bonds which are elongated with respect to the gas phase distance. The resulting geometry of the chemisorbed butenes is reminiscent of the structure obtained for propene adsorbed on Pt(1 1 1) [20]. In both cases, the unsaturated C=C bond lies nearly parallel to metal surface and the alkyl groups point outwards the surface.

3.2. Adsorption on Pd(1 1 1)

The characterisation of the adsorption (nature and strength) of 1,3-butadiene, 1-butene and 2-butenes on the Pd(1 1 1) surface has been carried out in parallel. Table 4 shows the adsorption energies calculated for the different molecules studied. As a general trend, one observes that the Pd surface clearly stabilises the π modes compared to the Pt one. For 1,3-butadiene the most favoured surface structure is again the 1,2,3,4-tetra-σ adsorption mode. Surprisingly, the binding energy is quite similar to the one obtained on the Pt surface despite the different geometrical parameters. The main structural details of the adsorption structures are given in Table 5. The diene molecule is much less distorted on the Pd(1 1 1) surface than on the Pt one and its geometry is closer to the gas phase, indicating that the molecule contains two activated double bonds rather than two di-σ type interactions. The terminal C–C bonds are only elongated by 0.11 Å and the C–CH_2 angle is now of ~144° (Table 5). This illustrates that the nomenclature π and σ is not directly related to the hybridisation of the organic molecule but to the nature of the molecule–surface interaction. Such a weakly distorted tetra-σ-adsorption mode with a remaining partial π character of the molecule can explain the NEXAFS results [6,27], which were previously assigned to a di-π mode. This weaker distortion of the molecular geometry on Pd(1 1 1) than on Pt(1 1 1) was observed in previous calculations carried out for the ethylene molecule [31]. To explain the same adsorption strength with such a different geometry, the decomposition of the adsorption energy in its main contributions have been performed. Fig. 4 shows the results we have obtained. When the molecule interacts with the metal surface new bonds are created and also the geometry of the molecule and the surface is modified. Hence, the adsorption energy is partitioned into the distortion energy of the molecule, distortion energy of the surface (minor contribution, not showed in the figure) and the interaction energy between the molecule and the surface. On the Pt(1 1 1) surface, the stronger distortion of the

Table 4
Adsorption energies (kJ mol^{-1}) for the various chemisorbed structures of 1,3-butadiene, 1-butene and 2-*cis*/*trans*-butene on Pd(1 1 1), as a function of the coverage

θ	1/3	1/4	1/6	1/9
1,3-butadiene				
di-π-*cis*				−138(−15)
di-π-*trans*			−123(−21)	−145(−16)
di-σ				−91(−10)
1,2−di-σ-3,4-π				−151(−17)
1,4−di-σ-2,3-π			−130(−22)	−154(−17)
1,2,3,4-tetra-σ			−145(−24)	−166(−18)
1-butene				
π	−25(−8)	−41(−10)	−62(−10)	−75(−8)
di-σ	−25(−8)	−57(−14)	−70(−12)	−87(−10)
2-cis-butene				
π				−64(−7)
di-σ				−74(−8)
2-trans-butene				
π				−56(−6)
di-σ				−69(−8)

The adsorption modes are those shown in Figs. 1 and 3. The values in parenthesis are the adsorption energies per surface metal atom.

Table 5
Geometrical parameters for the adsorption structures of 1,3-butadiene, 1-butene and 2-*cis*/*trans*-butene on Pd(1 1 1) for a coverage of $\theta = 1/9$-ML

	PdC_1	PdC_2	PdC_3	PdC_4	C_1C_2	C_2C_3	C_3C_4
1,3-butadiene							
di-π-*cis*	2.17	2.25	2.25	2.17	1.41	1.46	1.41
di-π-*trans*	2.18	2.22	2.22	2.18	1.41	1.45	1.41
di-σ	2.11	2.17	[2.81]	[3.64]	1.45	1.46	1.35
1,2-di-σ-3,4-π	2.11	2.19	2.34	2.15	1.45	1.45	1.42
1,4-di-σ-2,3-π	2.11	2.26	2.26	2.11	1.45	1.43	1.45
1,2,3,4-tetra-σ	2.12	2.23	2.25	2.11	1.45	1.45	1.45
1-butene							
π	2.20	2.22	[3.20]	[4.61]	1.40	1.51	1.54
di-σ	2.13	2.14	[2.98]	[4.98]	1.45	1.52	1.54
2-cis-butene							
π	[3.29]	2.24	2.24	[3.29]	1.50	1.41	1.50
di-σ	[2.99]	2.15	2.15	[2.99]	1.51	1.46	1.51
2-trans-butene							
π	[3.09]	2.23	2.23	[3.05]	1.51	1.41	1.51
di-σ	[2.98]	2.14	2.14	[2.98]	1.52	1.46	1.52

Distances are in Å. The numbers in brackets account for the longer distance between two atoms not directly bound.

molecule results in a higher energy cost to reach the adsorption geometry. On the other hand, the distortion favours the interaction between the molecule and the metal surface. Upon distortion the energy and shape of the molecular orbitals are modified. The distorted molecule has a higher lying occupied π orbitals and lower lying vacant ones which can develop stronger interactions with the vacant and filled surface electronic states respectively. However, the adsorbate–metal overlap is larger for Pt, since the d states are more expanded (see [31,56]). Consequently the stabili-

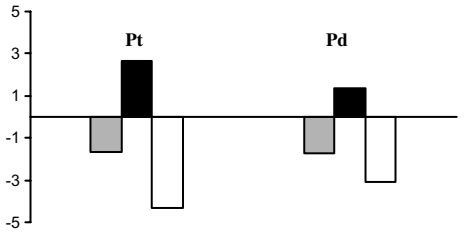

Fig. 4. Decomposition of the adsorption energy for the most stable adsorption mode (1,2,3,4-tetra-σ) on the Pt(1 1 1) and the Pd(1 1 1) surfaces. In the graphic from left to right: adsorption energy (light grey), distortion energy of the molecule (dark grey) and interaction energy between the molecule and the surface (white). Values in eV.

sation due to the molecule-surface interaction is more important on the Pt surface than on the Pd one. As the overall adsorption energy is a compromise between the distortion energy of the molecule and the stabilisation due to the interaction between the molecule and the metal surface, the higher energy cost to distort the molecule from its gas phase geometry on Pt(1 1 1) compared to the Pd surface results in a similar adsorption energy on both metal surfaces. This explains why the adsorption energy of 1,3-butadiene on the Pt and Pd(1 1 1) surfaces are similar, despite the fact that the adsorption geometries are quite different. Pt is clearly a case of strong interaction but also strong molecular distortion, while Pd shows a case of weaker interaction but resulting in an overall adsorption at least as efficient.

For all the butene isomers, the di-σ adsorption mode is the preferred one but the difference of stability with the π one is clearly smaller than on Pt(1 1 1) (Table 5). As in the case of the 1,3-butadiene molecule, the adsorption geometry is closer to the gas phase than on Pt(1 1 1) and the differences between the di-σ and π adsorption geometries are clearly smaller. Therefore, this moderately distorted di-σ structure on Pd keeps a partial π character for the C–C bond, in agreement with the experimental data. These experiments were previously associated to a π adsorption mode for the molecule [6,27], but they could be reinterpreted with a moderately distorted di-σ geometry. Differences between Pt and Pd are in agreement with the periodic trends found for the adsorption of ethylene on Pt-group metals [54] and rationalized using the πσ parameter [55] that increases from Pd to Pt, as the σ-bonding character increases. Additionally, the adsorbate–metal overlap measured as the adsorbate–metal d coupling-matrix element (2.78 for Pd, 3.90 for Pt) [56] results in an increased overlap with the adsorbate double bonds so that donation/back-donation is enhanced. Concerning the relative stabilities of butadiene and 1-butene, our calculations predict a considerable difference (79 kJ mol^{-1}) in the adsorption strength of the two molecules, favouring the butadiene. The free energy diagrams as a function of the temperature support this conclusion.

Calculations of the adsorption energy at different coverages have been performed for the 1-butene and the 1,3-butadiene molecules. If one considers the adsorption energy per surface unit, again the preferred surface structures are the 1,2,3,4-tetra-σ adsorption mode with a coverage of 1/6-ML for the 1,3-butadiene and the di-σ mode with a coverage of 1/4-ML for the 1-butene molecule.

4. Discussion and conclusion

Despite the different electronic behaviour of Pt and Pd surfaces, the same adsorption modes with close adsorption energies have been found for 1,3-butadiene and butenes on both metal surfaces. For the 1,3-butadiene molecule the preferred adsorption structure has been characterised as a tetra-σ mode with the four C atoms bounded to four neighbour Pt atoms. In this surface structure the carbon chain remains almost parallel to the surface. The most stable adsorption mode for the butenes is the di-σ-mode. In the optimised geometry the C=C bond lies parallel to the metal surface and the alkyl groups point outwards the surface. Nevertheless on Pd(1 1 1) the molecules are less distorted than on the Pt surface. Moreover, the π adsorption modes are less destabilised with respect to the σ ones on Pd(1 1 1). In consequence the energy difference between the di-σ and π modes is clearly smaller on palladium.

If the strength of the 1-butene adsorption is compared to that of 1,3-butadiene on Pt and Pd surfaces, only a small difference is observed. The

energy gap between the most stable adsorption modes for both molecules is 67 kJ mol^{-1} on Pt(1 1 1) vs. 79 kJ mol^{-1} on Pd(1 1 1). Therefore, it is difficult to only relate the different selectivity observed to this slight tendency of Pd to give a more facile butene desorption by competition with butadiene adsorption. It is not clear indeed why Pt could not give the same result. Consequently, to answer the problem of the selectivity, it seems to be necessary to go further in the study of the hydrogenation reaction itself. Preliminary results indicate that the different selectivity could rest on the relative stabilities of the reaction intermediates.

In conclusion, binding modes for 1,3-butadiene and butene isomers have been determined on Pt(1 1 1) and Pd(1 1 1). For 1,3-butadiene on Pt(1 1 1), combination of total energy calculations and simulations of the vibrational spectra allow us to determine the most favoured molecular adsorption mode as the 1,2,3,4-tetra-σ one and to reconcile the divergent proposals in the literature. On the Pd(1 1 1) surface, previous experimental works suggested a di-π adsorption mode. Calculations yield a σ-type interaction with moderate molecular distortion, which is fully compatible with the experimental results. For butenes, the calculations clearly point to a di-σ adsorption mode on both metal surfaces. From experiments, this was anticipated for Pt but not for the Pd surface where a π mode was predicted. Similarly to the case of the 1,3-butadiene molecule, the fact that molecular geometry is only slightly distorted upon adsorption on Pd(1 1 1) makes our results compatible with previous experimental results.

The present study shows that the different selectivity observed for the butadiene hydrogenation on Pt(1 1 1) and Pd(1 1 1) cannot be only explained by a competition between 1,3-butadiene and 1-butene. All these results provided us a good starting point for the study of the reactivity.

Acknowledgements

The authors thank David Loffreda for its assistance. They also thank the Institut du Développement et des Ressources en Informatique Scientifique (IDRIS) at Orsay (project 609) and the Centre Informatique National de l'Enseignement Supérieur (CINES) at Montpelier for CPU time. A.V. acknowledges financial support through the TMR activity "Marie Curie research training grants". Funding from the Spanish Ministerio de Ciencia y Tecnología (BQU2002-04029-CO2-01) and the Catalan Government (2001SGR00315) are also acknowledged. PS and FD thank P. Raybaud and F. Mittendorfer for helpful discussions.

References

[1] J. Cosyns, in: B. Imelik, G.A. Martin, A.J. Renouprez (Eds.), Catalyse par les Métaux, Edition du CNRS, Paris, 1984, p. 371.
[2] J. Massadier J.C. Bertolini, A. Renouprez, in: M.J. Phillips, M. Ternan (Eds.), Proc. 9th Int. Congress on Catalysis, Calgary, vol. III, 1988, p. 1222.
[3] T. Ouchaib, J. Massadier, A. Renouprez, J. Catal. 119 (1989) 517.
[4] C.-M. Pradier, E. Margot, Y. Berthier, J. Oudar, Appl. Catal. 43 (1988) 177.
[5] C. Yoon, M.X. Yang, G.A. Somorjai, Catal. Lett. 46 (1997) 37.
[6] G. Tourillon, A. Cassuto, Y. Jugnet, J. Massadier, J.C. Bertolini, J. Chem. Soc. Faraday Trans. 92 (1996) 4835.
[7] G. Pacchioni, R.M. Lambert, Surf. Sci. 304 (1994) 208.
[8] S. Cremer, X. Su, Y.R. Shen, G.A. Somorjai, J. Am. Chem. Soc. 118 (1996) 1926.
[9] F. Zaera, Langmuir 121 (1996) 88.
[10] A. Michalak, M. Witko, K. Hermann, J. Mol. Cat. A 119 (1997) 213.
[11] Q. Ge, D.A. King, J. Chem. Phys. 110 (1999) 4699.
[12] R.M. Watwe, R.D. Cortright, J.K. Norskov, J.A. Dumesic, J. Phys. Chem. B 104 (2000) 2299.
[13] L. Vattuone, Y. Yeo, R. Kose, D.A. King, Surf. Sci. 447 (2000) 1.
[14] A. Fahmi, R.A. Van Santen, J. Phys. Chem. 100–101 (1996) 5676.
[15] P.A. Sheth, M. Neurock, C.M. Smith, J. Phys. Chem. B 107 (2003) 2009.
[16] M. Neurock, V. Pallassana, R.A. van Santen, J. Am. Chem. Soc. 122 (2000) 1150.
[17] H. Steininger, H. Ibach, S. Lewald, Surf. Sci. 117 (1982) 685.
[18] C.E. Anson, N. Sheppard, B.R. Bender, J.R. Norton, J. Am. Chem. Soc. 121 (1999) 529.
[19] A. Valcárcel, J.M. Ricart, A. Clotet, A. Markovits, C. Minot, F. Illas, J. Chem. Phys. 116 (2002) 1165.
[20] A. Valcárcel, J.M. Ricart, A. Clotet, A. Markovits, C. Minot, F. Illas, Surf. Sci. 519 (2002) 250.
[21] M. Salmerón, G.A. Somorjai, J. Phys. Chem. 86 (1982) 341.

[22] R.J. Koestner, J.C. Frost, P.C. Stair, M.A. van Hove, G.A. Somorjai, Surf. Sci. 116 (1982) 85.
[23] N.R. Avery, N. Sheppard, Proc. R. Soc. Lond. A 405 (1986) 1.
[24] N.R. Avery, N. Sheppard, Proc. R. Soc. Lond. A 405 (1986) 27.
[25] M. Abon, J.C. Bertolini, B. Tardy, J. Chim. Phys. 85 (1988) 711.
[26] A. Cassuto, G. Tourillon, Surf. Sci. 307–309 (1994) 65.
[27] J.C. Bertolini, A. Cassuto, Y. Jugnet, J. Massardier, B. Tardy, G. Tourillon, Surf. Sci. 349 (1996) 88.
[28] Y. Tsai, B.E. Koel, J. Phys. Chem. B 101 (1997) 2895.
[29] R.C. Baetzold, Langmuir 3 (1987) 189.
[30] V. Maurice, C. Minot, Langmuir 5 (1989) 734.
[31] P. Sautet, J.-F. Paul, Catal. Lett. 9 (1991) 245.
[32] P. Hermann, D. Simon, P. Sautet, B. Bigot, J. Catal. 167 (1997) 33.
[33] F. Mittendorfer, C. Thomazeau, P. Raybaud, H. Toulhoat, J. Phys. Chem. B 107 (2003) 12287.
[34] G. Kresse, J. Hafner, Phys. Rev. B 47 (1993) 558.
[35] G. Kresse, J. Hafner, Phys. Rev. B 48 (1993) 13115.
[36] G. Kresse, J. Hafner, Phys. Rev. B 49 (1994) 14251.
[37] G. Kresse, D. Joubert, Phys. Rev. B 59 (1998) 1758.
[38] J.P. Perdew, Y. Wang, Phys. Rev. B 45 (1992) 13244.
[39] C. Morin, D. Simon, P. Sautet, J. Phys. Chem. B 107 (2003) 2995.
[40] D. Loffreda, Y. Jugnet, F. Delbecq, P. Sautet, J. Phys. Chem. B, submitted.
[41] Y. Morikawa, Phys. Rev. B 63 (2001) 033405.
[42] K. Reuter, M. Scheffler, Phys. Rev. B 65 (2001) 035406.
[43] W. Caminati, G. Grassi, A. Bauder, Chem. Phys. Lett. 148 (1988) 13.
[44] G.R. De Maré, Y.N. Panchenko, J. Vander Auwera, J. Phys. Chem. A 101 (1997) 3998.
[45] F. Delbecq, P. Sautet, J. Catal. 211 (2002) 398.
[46] F. Delbecq, P. Sautet, Catal. Lett. 28 (1994) 89.
[47] P. Ganis, I. Orabona, F. Ruffo, A. Vitagliano, Organometallics 17 (1998) 2646.
[48] J. Stöhr, F. Sette, A.L. Jonhnsons, Phys. Rev. Lett. 53 (1984) 1684.
[49] K.W. Wiberg, R.E. Rosenberg, J. Am. Chem. Soc. 112 (1990) 1509.
[50] M. Saeys, M.F. Reyniers, G.B. Marin, M. Neurock, Surf. Sci. 513 (2002) 315.
[51] A.P. Scott, L. Radom, J. Phys. Chem. B 100 (1996) 16502.
[52] G. Rauhut, P. Pulay, J. Phys. Chem. 99 (1995) 303.
[53] Complete data of the spectra are available upon request to the authors.
[54] N.F. Mrozek, M.J. Weaver, J. Phys. Chem. B 105 (2001) 8931.
[55] E.M. Stuve, R.J. Madix, J. Phys. Chem. 89 (1985) 3183.
[56] B. Hammer, J.J. Norskov, Adv. Catal. 45 (2000) 71.